

The Use of Bilinear Cohesive Zone Model to Study the Fracture of Mode I in Adhesive Joints

N. A. Yahya

Zawia University, Faculty of Engineering, Department of Mechanical and Industrial Engineering
Zawia, Libya
nyahya@zu.edu.ly

M. Lytwyn

University of Strathclyde, Faculty of Engineering, Department of Mechanical and Aerospace Engineering
Glasgow, United Kingdom

Abstract—Adhesively bonded joints can be numerically simulated using the Cohesive Zone Model (CZM) concepts. CZM are widely used for the strength prediction of adhesive joints. The critical strain energy release rate and critical interface strength are the parameters which must be known when cohesive elements in ABAQUS software are used. The formulation of the cohesive finite elements is based on the CZM approach with the bilinear traction-separation law. In this work, the parameters of two industrial adhesives Huntsman Araldite 2015 and resin LY3505/XB3405 for bonding of epoxy composites are identified. Double Cantilever Beam (DCB) test data was used for the identification. Finally, cohesive parameters are identified comparing numerically simulated load-displacement curves with experimental data retrieved from literature. Parametric study is performed to evaluate the variation of input parameters like initial stiffness, element size, peak stress and energy release rate 'G'. From the numerical evaluation, it was noted that CZM simulation relies largely on element size and peak cohesive strength.

Index Terms: Adhesively bonded composite, Mode I fracture, cohesive elements, bilinear traction-separation law, Araldite 2015.

I. INTRODUCTION

Adhesively bonded joints have very high utilization in different fields (e.g. automotive, aerospace, biomedical, microelectronics, etc). Adhesive joints provide several advantages over classical joining methods such as fastening or spot welding. Glued components transfer stresses more uniformly even if they are made of dissimilar materials, and a glued joint is lighter and less expensive than other traditional joining methods [1]. The increased application of the adhesive joints has been accompanied by the development of mathematical models to analyse the behaviour of these joints [2].

The use of so-called cohesive crack model for the modelling of the joints is one of the most appealing techniques. It has been developed since 1960s [3].

The aim of this work is the identification of the parameters of the cohesive crack model for two adhesives (Huntsman Araldite 2015 and resin LY3505/XB3405 for bonding of epoxy composites) applied on unidirectional carbon fiber reinforced composite modelled in the ABAQUS software [4].

The standard model used to describe the crack tip process zone assumes bonds stretching orthogonal to the crack surfaces until they break at a characteristic stress level. Thus, the singular region introduced from LEFM can be replaced by a lateral region over which non-linear phenomena occur. This model is often mentioned as the CZM and it can be traced back to the works of Dugdale and Barenblatt [5]. According to CZM the entire fracture process is lumped into the crack line and is characterized by a cohesive law that relates traction and displacement jumps across cohesive surfaces ($T-\Delta$). Unlike fracture mechanics based strategies, CZM can be used for the analysis of crack initiation and growth that, indeed, are obtained as a natural part of the solution without any a priori. So far, CZM has been successfully applied to model fracture in metals, concrete, polymers and functionally graded materials (FGMs) [6-10]. The sensitivity of the cohesive zone parameters (i.e. fracture strength and critical energy release rate) in predicting the overall mechanical response is first examined; subsequently, these parameters are tuned comparing numerically simulated load-displacement curves with experimental results retrieved from literature [11].

II. COHESIVE ZONE MODEL THEORY

The cohesive zone model regards fracture as a gradual phenomenon in which separation takes place across an extended crack 'tip', or cohesive zone and is resisted by cohesive tractions [12]. Thus cohesive zone elements do not represent any physical material, but describe the cohesive forces which occur when material elements (such as adhesive) are being pulled apart. Therefore cohesive zone elements are placed between the adherends and the implementation and calibrations of the models is mainly via FEM analysis. The main asset of this approach is that mixes the stress based approach used to model the elastic range with the energy fracture approach used to model the degradation of the adhesive properties.

Received 22 Sep, 2018; revised 30 Sep, 2018; accepted 4 Oct, 2018.

Available online Oct 6, 2018.

An alternative method to Linear Elastic Fracture Mechanics (LEFM) exists in the form of the cohesive zone modelling technique, which was first formulated by Dugdale and Barenblatt (1960 & 1962 respectively [5] [13]. This approach works by collating tractions (T) and displacement jumps (Δ) across cohesive surfaces on a crack line in which the fracture process has been combined onto. This relation works with the increase in separation across relative surfaces meaning an increase in traction before a maximum traction is obtained (peak cohesive strength, σ_0) which is then followed by a softening curve describing the post-peak behaviour, that eventually vanishes allowing for traction-free crack surfaces to be created [6]. The process of using cohesive zone models originates from the 1960's, however with the advances in modern FEM software this technique is gaining momentum in terms of applicability and use in the field of progressive damage mechanics. An important aspect to the successful implementation of a CZM involves the determination of the traction-separation relation used. This incorporates fracture parameters such as the fracture strength, σ_0 , and the relevant fracture energy which is specific to the mode of loading. Due to the complexities faced in trying to obtain accurate values for the respective peak strength and fracture energy, many workers in this field have opted to compare these fracture parameters with idealised numerical simulations in order to achieve a best fit [6],[14-16]. The most common traction-separation relations that have been developed are; the bilinear model, the exponential model and the trapezoidal model [6,17], as shown in Figure 1.

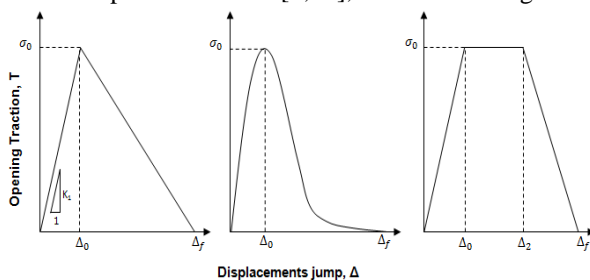


Figure 1. Schematic of i) Bilinear, ii) Exponential and iii) Trapezoidal

Where σ_0 represents the peak stress of the traction-separation relation, which has been argued to be of the same order as the tensile yield stress of the material used for the mode I loading case and this is something which will be analysed later in this research when considering the mode I loading of the DCB specimen [14]. The subsequent critical displacement jump at the peak stress is shown as Δ_0 , with the resultant failure point seen as Δ_f (for the trapezoidal relation an extra displacement point, Δ_2 , is added at the end point of an additional plateau in the softening region; which aims to capture the softening behaviour in more detail in order to represent the ductility of the material more adequately.

III. NUMERICAL ANALYSIS

For the analysis of the DCB experiment, begin by incorporating a solitary row of cohesive elements through the entire thickness of the adhesive (Araldite 2015) layer

or resin (LY3505/XB3405) layer. The intrinsic properties of the adhesive and the resin contained therein by means of the bilinear CZM. The properties of the Young's and shear moduli, strength of the bulk adhesive and resin matrix are based on data from relevant manufacturers and publications [11,18]. The measured fracture toughness are based on data was reported in [18]. Figure 2 shows the 2D model by the ABAQUS software where the adhesive is modelled as a row of cohesive elements. The fracture processes are assumed to occur within the adhesive. The adherends (mild steel) were modelled using bulk continuum elements i.e. 4-noded linear plane strain reduced integration continuum elements (CPE4R). The adhesive layer was modelled with a single row of 4-node cohesive elements (COH2D4) [4]. The von Mises stress distribution and the damage propagation are shown in Figure 3 and Figure 4 respectively.

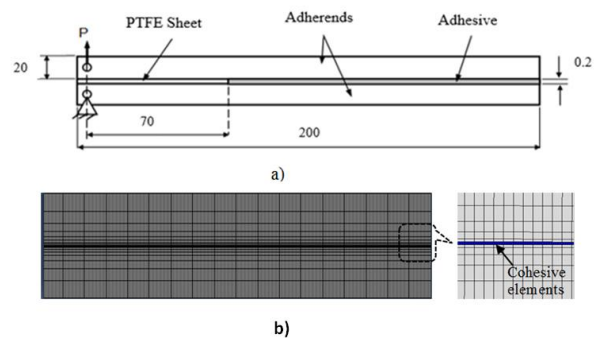


Figure 2. a) Geometry and Dimensions (in mm) of the DCB Model and Boundary Conditions and b) DCB Mesh used with Single Row of Cohesive Elements to Represent the Adhesive Thickness

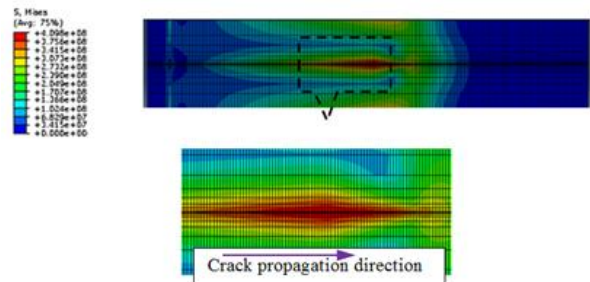


Figure 3: The Von Mises Stress Distribution of DCB Mesh after Crack Propagation in the Adhesive

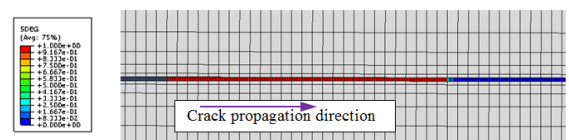


Figure 4: Damage Predictions by Finite Element Model Using the CZM

IV. RESULTS AND DISCUSSION

A. Effects of Cohesive Parameter

The numerical analysis of the DCB with a study on the effect of varying the normal peak strength of the bilinear, CZM used through means of tailoring this model with experimental data. A sensitivity study is then performed

on this mode I fracture parameter. Also in order to gain a suitable best fit to the experimental data, which is then followed by searching for an optimal cohesive element length. Then subsequently analysing the effects of varying all other relevant parameters involved and thus monitoring the load-displacement curve in each case as a reference.

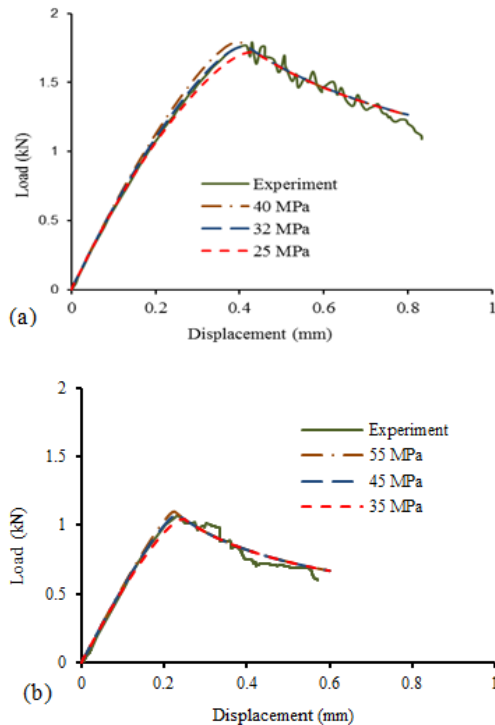


Figure 5: Study on Effect of Varying Normal Strength of (a) Araldite 2015 and (b) Resin LY3505/XB3405

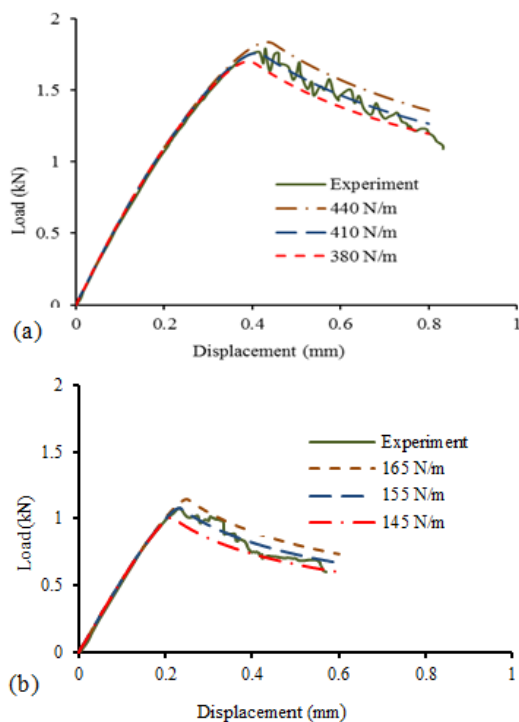


Figure 6: Study on the Effect of the Varying Mode I Fracture Energy of (a) Araldite 2015 and (b) Resin LY3505/XB3405

The data fit achieved in Figures 5 and 6 are results of iteratively adjusting the peak strength and fracture energy of the bilinear CZM until an acceptable match with the experimental plot was achieved. The cohesive parameters used are those in which give rise to the minimum deviation between experimental and numerical simulations and are summarised in Table 1.

Table 1. Cohesive Parameters Deduced from Data Fitting for Mode I

Material	GIC (N/m)	σ (MPa)
Araldite 2015	410	32
Resin LY3505/XB3405	155	45

B. Effects of Cohesive Zone Length

Another important factor in the numerical simulation of delamination is the length of the cohesive zone, L_{CZ} . As opening displacement increases, elements in the cohesive zone gradually reach the maximum interfacial strength and the maximum stress rises up to the critical interfacial stress ahead of the crack tip. The length of the cohesive zone, L_{CZ} , is defined as the distance from the crack tip to the point where the maximum cohesive traction is reached. Figure 7 describes the length of the cohesive zone.

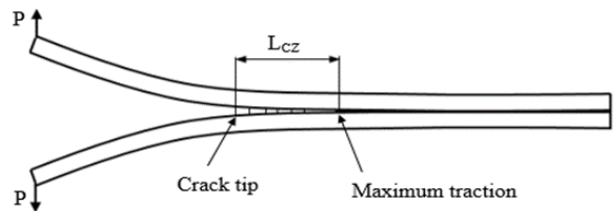


Figure 7: Length of the Cohesive Zone

There are a number of different models that have been used in different literature, but the most commonly used models are Hillerborg’s model and Rice’s model. For Mode I fracture the cohesive length can be compute by the following equation.

$$L_{CZ}^I = ME \frac{G_{IC}}{\sigma^2} \tag{1}$$

Where E is the Young’s modulus and M is a parameter that depends on the cohesive zone theory used to determine the cohesive zone length. Different M values are given in Table 2.

Table 2. Different Values of the Parameter M in Literature [4]

Proposed by:	M
Dugdale and Barenblatt	0.40
Rice and Flak et. al.	0.88
Hillerborg et al.	1.00

The length of the cohesive elements can be calculated from the following equation for Mode I:

$$L_e = \frac{L_{CZ}^I}{N_e} \tag{2}$$

Where N_e is the number of elements and L_e is the length of the cohesive element.

The cohesive zone length is directly related to the convergence issue that is the most crucial point for the CZM applications. Turon et al. [10] suggested that the minimum number of elements required for reaching converged solutions should be more than two. Therefore the resulting element length can be given as;

$$L_e \leq \frac{L_{CZ}}{3} \tag{3}$$

From the inverse identification procedure, it is apparent that a cohesive strength of $\sigma = 32$ MPa and a mode I fracture energy of $GIC = 410$ N/m returns the optimal solution in terms of correlating this model with the experimental DCB test. Using these values, we can therefore proceed to compute an estimate of the actual cohesive zone length in the numerical DCB model using above equation.

As mode I is the fracture mode; M is a parameter ranging from 0.21 to 1.0 [12]. For Araldite 2015, $E = 1.8$ GPa, and using the fracture energy and cohesive strength values for Mode I from Table 2, we can find the length of the fracture process zone in Mode I as; $0.15 \text{ mm} < L_{CZ} < 0.72 \text{ mm}$ (by using $M = 0.21$ and 1.0 respectively). Many workers in this area have stipulated that in order to accurately characterise the cohesive zone (L_{CZ}), one must use at least 3 cohesive elements along the fracture process zone [6, 12]. The parameter M is of some ambiguity, as this value is used to gain an estimate of the cohesive zone, derived from methods such as estimating L_{CZ} as a function of crack growth velocity or estimating the size of the yield zone ahead of a mode I crack. It is common for M to equal unity, but this may add a degree of conservatism to the analysis. One method of investigating the length of the numerically predicted cohesive zone length is, for instance, by placing very fine (0.01 mm) cohesive elements along the length of the DCB bondline, then analysing the S22 (peel) stress ahead of the crack tip at the corresponding peak value of force (from the load-displacement plot found using 0.01 mm cohesive elements) [12].

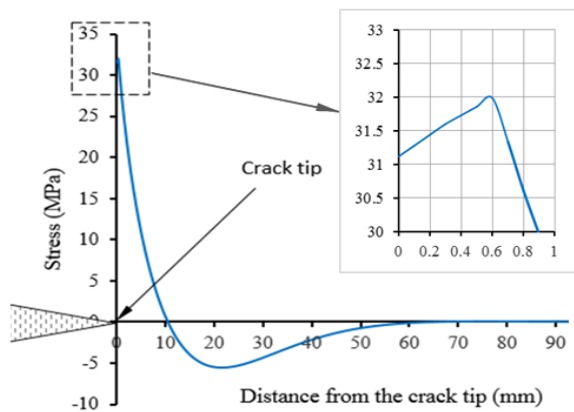


Figure 8: Illustration of S22 Traction Ahead of Crack Tip, with Very Fine Mesh Used to Capture Cohesive Zone Length

A preliminary investigation into this procedure has been conducted and illustrated in Figure 7, allowing for an accurate estimation of the numerically predicted cohesive zone length to be found for the DCB geometry

used in this work. The S22 stress magnitudes obtained here are from the peak load (1640 N), and one can observe that the peak traction reached behind the crack tip will not exceed the cohesive strength set in the intrinsic bilinear CZM relation utilised here.

In order to obtain the accurate results, the tractions in the cohesive zone must be represented properly by the finite element spatial discretisation and as such this can be illustrated as:

$$N_e = \frac{L_{CZ}}{L_e} \tag{4}$$

Where N_e is the number of cohesive elements in the cohesive zone.

In Figure 8 the peak normal stress occurs at 0.6 mm from the crack tip and so the cohesive zone length, L_{CZ} is approximately 0.6 mm. Although this method is not precise, it does give a good estimate to the cohesive zone length.

C. Investigation of Mesh Refinement

In order to investigate the effect of mesh refinement in the cohesive zone length on numerical prediction of delamination onset, several DCB specimens were simulated with different lengths of cohesive elements in the cohesive zone length. Figure 9 shows the results of a sensitivity study on the cohesive element length against the resulting numerical load-displacement response.

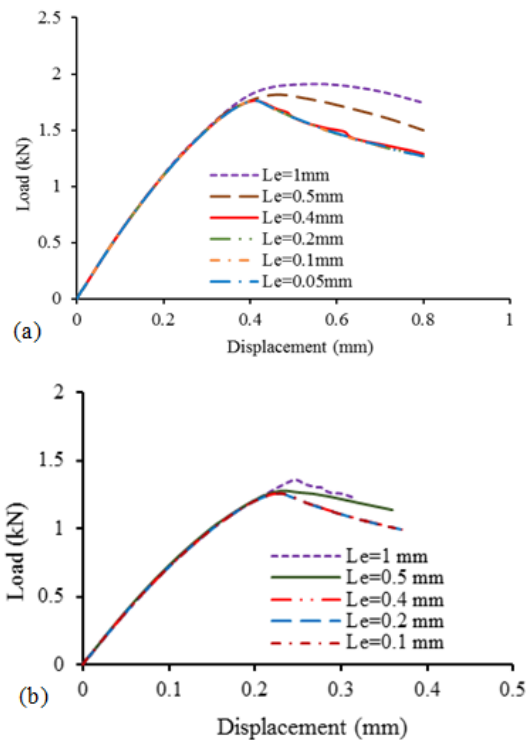


Figure 9: The Effect of Cohesive Element Length on the Predicted Load-Displacement Curve of (a) Araldite 2015 and (b) Resin LY3505/XB3405.

The results illustrate that for all mesh sizes a converged solution was obtained but it is necessary to apply a mesh size, L_e , less than 0.2 mm to accurately predict delamination initiation. A good model usually consists of 3 or 4 elements within the cohesive zone length. In the

current study, cohesive element length, L_e is initially chosen to be 0.2 mm. By bisecting the element length in subsequently refined meshes along the crack path, L_e finally equals 0.05 mm in the most refined mesh of DCB model.

V. CONCLUSIONS

Parameters of two adhesives (Araldite 2015 and epoxy resin LY3505/XB3405), which are necessary for modelling of bonded joints. The cohesive zone model in the form of the bilinear relation, were identified. To describe the joint behavior after the first failure more precisely, the critical strain energy release rate should have different values in the cohesive elements that represent the initial location of the crack and in the rest of cohesive elements.

A numerical study was carried out including a bilinear cohesive damage model to simulate the behaviour of adhesive and epoxy resin. An inverse method was used to define the remaining cohesive parameters of the bilinear relation, fitting the numerical and experimental load-displacement curves. This was done by comparing the peak force of the experimental load-displacement plot with the numerical output of the DCB model, until a minimum deviation between the two plots was observed. The peak strength was obtained by using a very fine cohesive element length (0.01 mm) in order to accurately capture tractions in the cohesive zone of the numerical model. Numerical analysis with different discretization of the cohesive zone length showed that numerical predicted responses correlate well with the experimental solutions when at least 3 elements span the cohesive zone length. Cohesive modelling has an advantage in showing failure initiation and propagation. The value of scalar stiffness degradation (SDEG) in the cohesive zone can be employed to show the joint failure history, and used to display the behavior of the interfacial element are shown in Figure 4. Regarding the numerical model can be further enhanced to consider the thick-bondline formulations. The effects of the size of bonding area on steel-composite joints and on composite-composite joints should also be investigated as not only steel adherends are used in engineering applications. Also the concept of CZM's are very recent and need further validations and improvements for a widespread application to different geometries and load conditions.

REFERENCES

- [1] R.D.S.G. Campilho, M.F.S.F. de Moura, and J.J.M.S. Domingues, "Modelling single and double lap repairs on composite materials," *Composites Science and Technology*, vol. 65, p. 1948–1958, 2005.
- [2] G.R. Wooley, and D.R. Carver, "Stress concentration factors for bonded lap joint," *Journal of Aircraft*, vol. 8, p. 817–820, 1971.
- [3] J.A. Harris, and R.D. Adams, "Strength prediction of bonded single lap joints by nonlinear finite element methods," *International Journal Adhesion and Adhesives*, vol. 4, pp. 65-78, 1984.
- [4] N.A. Yahya, and S.A. Hashim, "Stress analysis of steel/carbon composite double lap shear joints under tensile loading," *Proc IMechE Part L: Journal of Materials: Design and Applications*, vol. 230, no. 1, p. 88–104, 2016.
- [5] L.F.M. da Silva, R.J.C. Carbas, G.W. Crichtlow, M.A.V. Figueiredo, and K. Brown, "Effect of material, geometry, surface treatment and environment on the shear strength of single lap joints," *International Journal Adhesion and Adhesives*, vol. 29, pp. 621-632, 2009.
- [6] S. Feih, and H.R. Shercliff, "Adhesive and composite failure prediction of single-L joint structures under tensile loading," *International Journal Adhesion and Adhesives*, vol. 25, pp. 47-59, 2005.
- [7] R.A. Odi and C.M. Friend, "An improved 2D model for bonded composite joints.," *International Journal of Adhesion and Adhesives*, vol. 24, pp. 389-405, 2004.
- [8] M.D. Aydin, A. Özel, and S. Temiz, "Non-linear stress and failure analyses of adhesively-bonded joints subjected to a bending moment," *Journal of Adhesion Science and Technology*, vol. 18, p. 1589–1602, 2004.
- [9] B.B. Bachir, B. Achour, M. Berrahou, D. Ouinas, and X. Feaugas, "Numerical estimation of the mass gain between double symmetric and single bonded composite repairs in aircraft structures," *Material and Design*, vol. 31, p. 3073–3077, 2010.
- [10] A.G. Magalhaes, M.F.S.F. de Moura, and J.P.M. Gonçalves, "Evaluation of stress concentration effects in single-lap bonded joints of laminate composite materials," *International Journal of Adhesion and Adhesives*, vol. 25, pp. 313-319, 2005.
- [11] S. Akpınar, "Effects of laminate carbon/epoxy composite patches on the strength of double-strap adhesive joints: Experimental and numerical analysis," *Materials and Design*, vol. 51, p. 501–512, 2013.
- [12] R.D. Adams, J. Comyn, and W.C. Wake, *Structural adhesive joints in engineering*, Dordrecht: Kluwer Academic Publishing, 1997.
- [13] ESA PSS-03-203, *Structural Materials Handbook*, Issue 1, Vol 1. 1994 [Chapter 21].
- [14] R.D. Adams, R.W. Atkins, J.A. Harris, and A.J. Kinloch, "Stress analysis and failure properties of carbon fibre reinforced plastic steel double lap joints," *Journal of Adhesion*, vol. 20, p. 29–53, 1986.
- [15] T. Schjelderup, and C.G. Gustafson, "The wedge test approach to mode I interlaminar fracture toughness for CFRP," in *Proceedings of the 6th European Conference on Composite Materials*, September 20–24, 1993.
- [16] V. Pocius, *Adhesion and Adhesive Technology*, An Introduction Alphonse, ISBN 1-56990-212-7, 1997.
- [17] S.A. Hashim et al., "Fabrication, testing and analysis of steel/composite DLS adhesive joints," *Ships and Offshore Structures*, vol. 6, no. 1-2, pp. 115-126, 2011.
- [18] "Huntsman Advanced Materials," www.huntsman.com, 2004".
- [19] N.A. Yahya, and S.A. Hashim, "Delamination of thick adherend steel/CFRP laminate connections," in *The European Adhesion Conference (9th EURADH)*, Friedrichshafen/Germany, September 2012.
- [20] Z. Wu, "Stress concentration analyses of bi-material bonded joints without inplane stress singularities," *International Journal of Mechanical Sciences*, vol. 50, pp. 641-648, 2008.
- [21] S.A. Hashim, M.J. Cowling, and S. Lafferty, "The integrity of bonded joints in large composite pipes," *International Journal of Adhesion and Adhesives*, vol. 18, pp. 421-429, 1998.